Journal of Achievements in Materials and Manufacturing Engineering
VOLUME 61
ISSUE 2
December
2013

Defects in the structure of $Fe_{60}Co_{10}W_2Me_2Y_8B_{18}$ amorphous metallic glasses, where Me=(Mo,Nb)

S. Garus [a,*], J. Garus [a], M. Nabiałek [a], K. Błoch [a], K. Gruszka [a], M. Szota [b]
[a] Institute of Physics, Technical University of Częstochowa,
ul. Armii Krajowej 19, 42-200 Częstochowa, Poland
b Institute of Materials Engineering, Technical University of Częstochowa,
ul. Armii Krajowej 19, 42-200 Częstochowa, Poland
* Corresponding e-mail address: gari.sg@gmail.com

Received 14.10.2013; published in revised form 01.12.2013

Materials

ABSTRACT

Purpose: The paper presents results of the effect of structural defects on the process of magnetization in high magnetic fields in metallic glasses based on amorphous $Fe_{60}Co_{10}W_2Me_2Y_8B_{18}$ (where Me=Mo, Nb)
Design/methodology/approach: Bulk amorphous material samples were obtained with the method of rapid radial cooling in the copper liquid-cooled mould in a protective atmosphere of inert gas. The samples in the state after solidification were then examined using a vibrating magnetometer in the magnetic fields up to 2T. Static magnetic hysteresis loops and primary magnetization curve were recorded.
Findings: Changing a small amount of the element from the group of transition metals have a significant effect on the magnetic properties of the produced alloy. Depending on the substituent also the type of defects identified in the examined materials changes.
Research limitations/implications: It is advisable to conduct studies on samples with compositions close to studied in this work for better prediction of magnetic properties of materials.
Practical implications: Bulk amorphous metallic glass are used in the electrical industry as cores in modern high-efficiency high-power transformers.
Originality/value: W Paper presents studies on the influence of structure defects on the process of primary magnetization for amorphous $Fe_{60}Co_{10}W_2Mo_2Y_8B_{18}$ and $Fe_{60}Co_{10}W_2Nb_2Y_8B_{18}$ alloys. Alloys of given composition has not yet been tested for the influence of defects on the magnetization process.
Keywords: Amorphous materials; metallic glasses; Magnetic properties; Structure defects

Reference to this paper should be given in the following way:
S. Garus, J. Garus, M. Nabiałek, K. Błoch, K. Gruszka, M. Szota , Defects in the structure of $Fe_{60}Co_{10}W_2Me_2Y_8B_{18}$ amorphous metallic glasses, where Me=(Mo, Nb), Journal of Achievements in Materials and Manufacturing Engineering 61/2 (2013) 175-180.

1. Introduction

The H. Kronmuler method allows the determination of the structural defects occurring in amorphous materials [1-6]. As is known, internal stresses created during the rapid cooling during the manufacture of the bulk amorphous alloys, cause local density fluctuations, and thus have a significant influence on the magnetic properties of these materials [1,4,6,7]. Due to the presence of local density inhomogeneities, these materials are characterized

by a greater energy in the state after solidification, and while trying to minimize energy, the spontaneous transition to the crystalline state occurs. This process takes place even at relatively low temperatures (e.g. at room temperature, but the time it takes to transition from the amorphous to the crystalline state is sufficiently long). The intensity of this process depends both on the heat treatment conditions and the chemical composition of the alloy. For this reason, it is believed that the amorphous state is a metastable state.

Density fluctuations manifest themselves by the occurrence of point defects and their linear conglomerates, called quasi-dislocation dipoles, which are present in the sample volume. If in the amorphous material structural defects are present, the difference between the saturation magnetization and the magnetization of the sample can be defined as follows:

$$\Delta M = \Delta M_{ins} + \Delta M_{para} + \Delta M_{def} \tag{1}$$

where ΔM_{ins} is caused by internal fluctuations (local differences in in density, anisotropy) which can be omitted because of its small contribution [1, 4], ΔM_{para} is associated with the external magnetic field in the internal spin waves damping phenomenon, and for the ΔM_{wew} defects within the structure of the metallic glass is responsible.

To describe the magnetization in strong magnetic fields for amorphous materials, theory called approach to ferromagnetic saturation is used, because of the good representation of the experimental data. [4, 6, 8]. Near the point defects deformation occurs towards the magnetization vector, and in the case of quasi-dislocation dipoles there is an attachment of magnetization deformation centers, which show non collinear character.

Analysis of the shape of the magnetization curve as a function of the strong magnetic field allows to determine the type of defects present in the material by the relationship:

$$\mu_0 M(H) = \mu_0 M_s \left[1 - \frac{a_{1/2}}{(\mu_0 H)^{1/2}} - \frac{a_1}{(\mu_0 H)^1} - \frac{a_2}{(\mu_0 H)^2} \right] + b(\mu_0 H)^{1/2} \tag{2}$$

where μ_0 - permeability of vacuum; H- magnetic field intensity; M_s - spontaneous magnetization; a_i - the directional coefficients of the linear fit (responsible for the free volume and linear defects; i=1/2,1,2); *b*- directional factor for linear fit corresponds to the damping of thermally excited spin waves by a magnetic field - Holstein-Primakoff paraprocess [9].

The analysis is performed by designating factors $a_i/(\mu_0 H)^i$. They describe the deviation from the saturation magnetization, which is caused by non-uniformity of local polarization vectors.

The free volume, the equivalent of vacancies in the crystal lattice parameter affect on the $a_{1/2}/(\mu_0 H)^{1/2}$ parameter, which can be defined as [5, 6]

$$\frac{a_{1/2}}{(\mu_0 H)^{1/2}} = \mu_0 \frac{3}{20 A_{ex}} \left(\frac{1+r}{1-r} \right)^2 G^2 \lambda_s^2 (\Delta V)^2 N \left(\frac{2A_{ex}}{\mu_0 M_s} \right)^{1/2} \frac{1}{(\mu_0 H)^{1/2}} \tag{3}$$

where N - bulk density of point defects; ΔV- volume change evoked by point defects; A_{ex}- exchange constant; *r* - Poissons factor; G- elastic shear modulus; λ_s- saturation magnetization.

Occurrence of factors $\frac{a_1}{(\mu_0 H)}$ and $\frac{a_2}{(\mu_0 H)^2}$ described by [4,10]:

$$\frac{a_1}{(\mu_0 H)} = 1{,}1 \mu_0 \frac{G^2 \lambda_s^2}{(1-V)^2} \frac{N b_{eff}}{M_s^2} D_{dip}^2 \frac{1}{(\mu_0 H)^2} \tag{4}$$

and [4, 10]:

$$\frac{a_2}{\mu_0 H} = 0{,}456 \mu_0 \frac{G^2 \lambda_s^2}{(1-V)^2} \frac{N b_{eff}}{M_s^2} D_{dip}^2 \frac{1}{(\mu_0 H)^2} \tag{5}$$

where D_{dip}- width of the dipoles; *N*- bulk density; b_{eff}- effective Burgers vector, is due to the presence of conglomerates of free volumes (linear defects) in the amorphous structure. The first occurs when the width of the dipole D_{dip}- is related to the inverse of the exchange distance l_H [2,5,6] by dependence $l_H^{-1} D_{dip} < 1$, where

$$l_H = \left(\frac{2A_{ex}}{\mu_0 H M_s} \right)^{1/2} \tag{6}$$

Exchange distance A_{ex} is related to D_{spf} by dependence [4, 11]

$$A_{ex} = \frac{M_s D_{spf}}{2 g \mu_B} \tag{7}$$

In the second case, where $l_H^{-1} D_{dip} > 1$ the dominant becomes the factor $\frac{a_2}{(\mu_0 H)^2}$.

Above the limit value of the field H_p[T] structural defects no longer have effect on the process of magnetization. In this area, the magnetization can be described by the relationship $b(\mu_0 H)^{1/2}$. Then damping of thermaly excited spin waves by the external magnetic field occurs - there is the Holstein-Primakoff process

2. Research

The study investigated the effect of Me=(Mo, Nb) on the type of defects in the structure of the bulk $Fe_{60}Co_{10}W_2Me_2Y_8B_{18}$ amorphous alloys. Ingots of these alloys obtained by arc melting of the high purity components of several times in a protective atmosphere of argon, in order to ensure maximum uniformity of the distribution of the individual components throughout the volume of the sample. The amorphous plates were made by injection under pressure to a liquid-cooled copper mold, in which

the radial cooling of the liquid material occured. This process also took place in a protective atmosphere of argon.

Studies of magnetization in the strong magnetic field were performed using the LakeShore vibration magnetometer (VSM) in the fields range from 0 to 2T for the samples in the state after solidification.

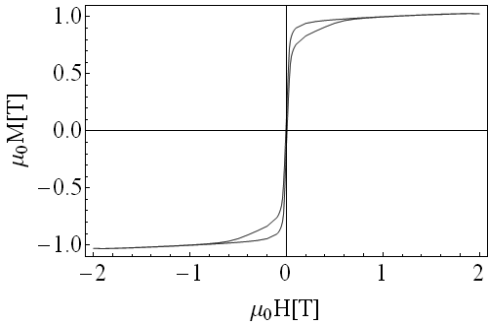

Fig. 1. Hysteresis loop for the $Fe_{60}Co_{10}W_2Mo_2Y_8B_{18}$alloy in the as-quenched state

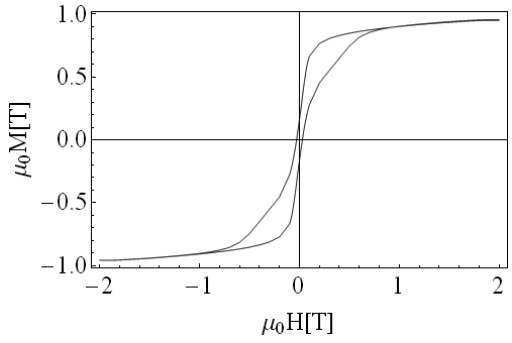

Fig. 2. Hysteresis loop for the $Fe_{60}Co_{10}W_2Nb_2Y_8B_{18}$ alloy in the as-quenched state

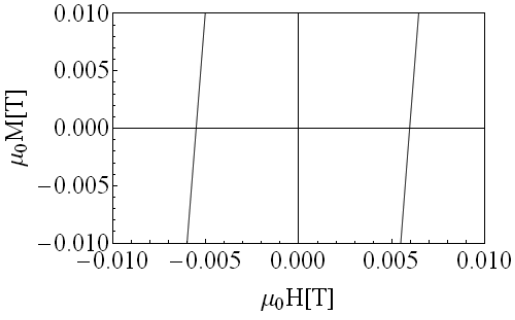

Fig. 3. Coercivity field for the $Fe_{60}Co_{10}W_2Mo_2Y_8B_{18}$ alloy

Figs. 1 and 2 respectively show the static hysteresis loops for $Fe_{60}Co_{10}W_2Mo_2Y_8B_{18}$ alloy and $Fe_{60}Co_{10}W_2Nb_2Y_8B_{18}$, whereas in Figs. 3 and 4 fragment closeups are presented to allow the determination of coercive field. The initial magnetization curve of a sample doped with Mo is shown in Fig. 5, while the Nb dopant curve is shown in Fig. 6.

As can be seen, the static hysteresis loops have the wasp-like shape, probably caused by blurr of the amorphous matrix. The nature of the curves and the relatively small area of coercivity, are typical of the so-called soft magnetic properties material. Since the area of the hysteresis loop is directly proportional to the magnetization losses, it is expected that the alloy with the addition of Mo will have better magnetic properties. Saturation magnetization of the sample was 1.0286 Mo [T] while the sample with Nb was 0.9516 [T].

Coercivity field for a sample with Mo is Hc = 5.7 [mT] while the sample with the addition of Nb, has coercivity field almost five times larger and is Hc = 29 [mT].

In Figs. 5 and 6 shows the the initial magnetization curves for investigated samples, respectively $Fe_{60}Co_{10}W_2Mo_2Y_8B_{18}$ and $Fe_{60}Co_{10}W_2Nb_2Y_8B_{18}$.

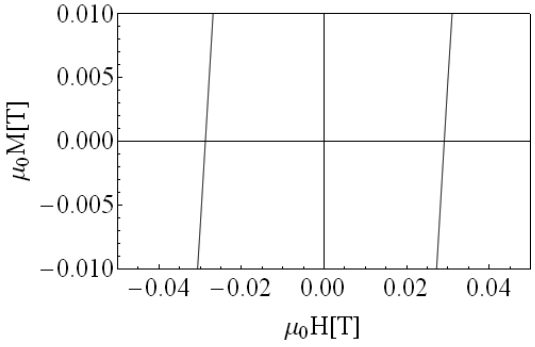

Fig. 4. Coercivity field for the $Fe_{60}Co_{10}W_2Mo_2Y_8B_{18}$alloy

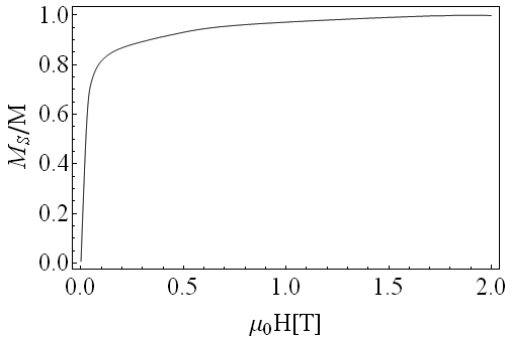

Fig. 5. Initial magnetization curve for $Fe_{60}Co_{10}W_2Mo_2Y_8B_{18}$.

According to the Kronmüller theory magnetization curve analysis was carried, where the influence of point and line defects of type I and II on the process of magnetization for various ranges of $\mu_0 H$.

Results of the analysis of these curves is shown in Table 1. By providing the reduced magnetization M/M_S in function of $1/(\mu_0 H)^{1/2}$, $1/(\mu_0 H)$, $1/(\mu_0 H)^2$, or $(\mu_0 H)^{1/2}$ linear fit was possible using the method of least squares.

On Figs. 7-9, high field magnetization curves are shown for the $Fe_{60}Co_{10}W_2Mo_2Y_8B_{18}$ alloy.

The linear dependence of the reduced magnetization from $(\mu_0 H)^{-1/2}$ (Fig. 7) in the field range from 0.054 T to 0.42 T indicates that in this respect the process of magnetizing is associated with the rotation of the magnetic moments near the point defects. In fields from 0.42 T to 0.86 T were observed linear dependence of the reduced magnetization as a function of $(\mu_0 H)^{-1}$ (Fig. 8). In this range of the magnetic fields, on the sample magnetization most influence had line defects, so-called quasi-dislocation dipoles. Further increase of the magnetization for $(\mu_0 H)$> 0.86 T is associated with damping of thermally excited spin waves by a magnetic field, (Fig. 9).

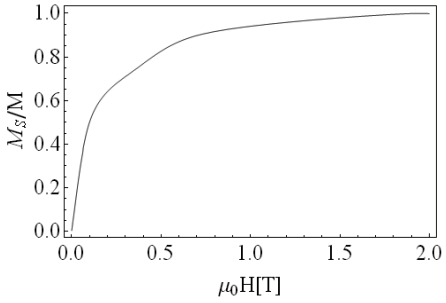

Fig. 6. Initial magnetization curve for $Fe_{60}Co_{10}W_2Nb_2Y_8B_{18}$.

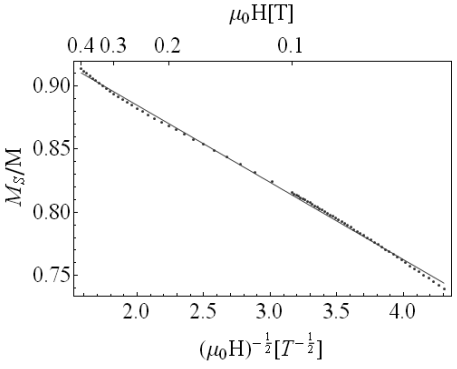

Fig. 7. Magnetization $Fe_{60}Co_{10}W_2Mo_2Y_8B_{18}$ in function of $(\mu_0 H)^{-1/2}$

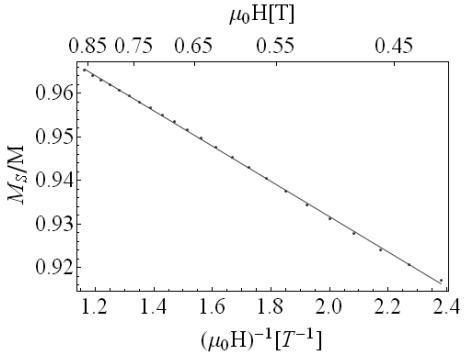

Fig. 8. Magnetization of $Fe_{60}Co_{10}W_2Mo_2Y_8B_{18}$ in function of $(\mu_0 H)^{-1}$

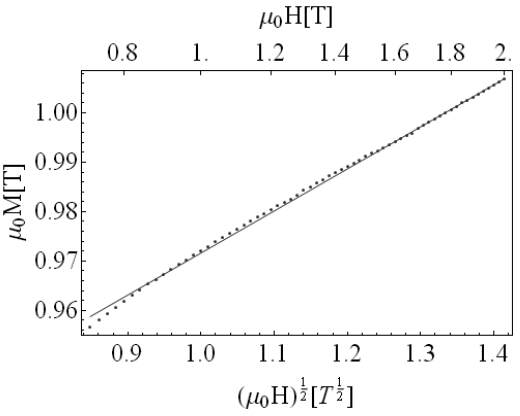

Fig. 9. Magnetization of $Fe_{60}Co_{10}W_2Mo_2Y_8B_{18}$ in function of $(\mu_0 H)^{1/2}$

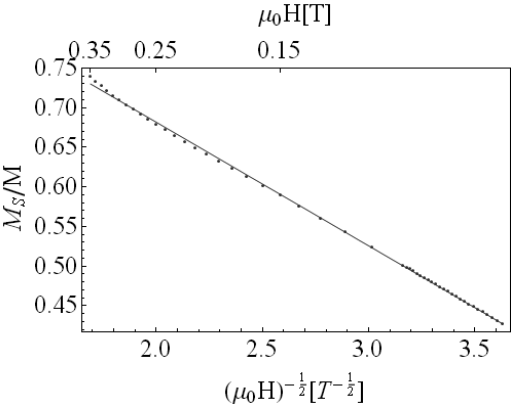

Fig. 10. Magnetization of $Fe_{60}Co_{10}W_2Nb_2Y_8B_{18}$ in function of $(\mu_0 H)^{-1/2}$

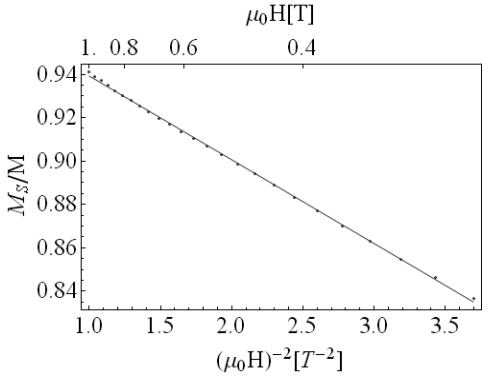

Fig. 11. Magnetization of $Fe_{60}Co_{10}W_2Nb_2Y_8B_{18}$ in function of $(\mu_0 H)^{-2}$

In the case of the $Fe_{60}Co_{10}W_2Nb_2Y_8B_{18}$ alloy also observed a linear relationship of $M/M_s((\mu_0 H)^{-1/2})$ in field range from 0.08 T to 0.35 T (Fig. 10), which indicates the presence of point defects

in the sample. In field range from 0.35 T to 1 T on magnetization process linear defects influenced, as evidenced by the reduced linear dependence of the magnetization $(\mu_0 H)^{-2}$ (Fig. 11). At higher magnetic fields above 1 T, as in the previous alloy, Holstein-Primakoff process was observed (Fig. 12).

Results of the analysis of high-field magnetization curves are summarized in Table 1.

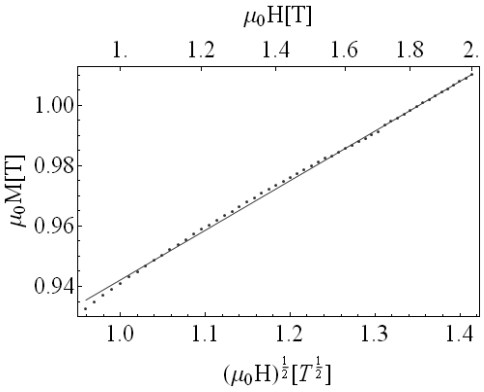

Fig. 12. Magnetization of $Fe_{60}Co_{10}W_2Nb_2Y_8B_{18}$ in function of $(\mu_0 H)^{1/2}$

Table 1.
Data obtained from the analysis of magnetization as a function of magnetic field to the powers of: -½, -1, -2 and ½

	$Fe_{60}Co_{10}W_2Mo_2Y_8B_{18}$	$Fe_{60}Co_{10}W_2Nb_2Y_8B_{18}$
$H_c[mT]$	5.7	29
$b\left[10^{-2}T^{-1/2}\right]$	0.08508	0.16418
$a_2\left[T^{-2}\right]$	-	0.0386076
$a_1\left[T^{-1}\right]$	0.04046	-
$a_{1/2}\left[T^{-1/2}\right]$	0.0610937	0.15607
$M_S[T]$	1.0286	0.951676
$\mu_0 H_p[T]$	0.86	1
$D_{spf}\left[meV\cdot nm^2\right]$	34.34	22.15
$D_{dip}\left[10^{-1}nm\right]$	18.2	-
$A_{dex}\left[10^{-12}\frac{J}{m}\right]$	1.16	0.69
$N_{dip}\left[10^{16}m^{-2}\right]$	30.1	-

Subsequent row of the table means H_c - coercivity, b - directional coefficient for fit of power ½, a_2 - directional coefficient for fit of power -2, a_1 - directional coefficient for fit of power -1, $a_{½}$ - directional coefficient for fit of power -½, M_s - saturation magnetization, $\mu_0 H_P$ - eld, above which is observed paraproces, D_{spf} - spin-wave stiffness parameter, D_{dip} – width of the dipolesA$_{dex}$ - exchange coefficient, N_{dip} - density of quasidislocational dipoles.

For the amorphous $Fe_{60}Co_{10}W_2Mo_2Y_8B_{18}$ alloy conglomerates of linear defects occurred of type I, which allowed the determination of the density N_{dip} of those defects. For the $Fe_{60}Co_{10}W_2Nb_2Y_8B_{18}$ sample, due to the large number of conglomerates of type II, linear defect density of structural defects designation was not possible.

3. Conclusions

In this work, the influence of defects on the process of the magnetization for the amorphous $Fe_{60}Co_{10}W_2Mo_2Y_8B_{18}$ and $Fe_{60}Co_{10}W_2Nb_2Y_8B_{18}$ alloys was studied. The static hysteresis loops characters indicate, that the samples were soft magnetic amorphous alloys. Exchange Mo by Nb dopant has increased the coercive field and caused the reduction of saturation magnetization. It should be noted for the occurrence of inwar effect in alloy containing Nb.

In the studied amorphous alloys magnetization in strong fields affect both point defects and quasi-dislocation dipoles. However, a decisive role in the process of magnetization of amorphous $Fe_{60}Co_{10}W_2Mo_2Y_8B_{18}$ alloy the greatest role plays the conglomerate of free volume of type I, while in alloy $Fe_{60}Co_{10}W_2Nb_2Y_8B_{18}$ magnetization process is related to the second type of linear defects.

References

[1] M. Born, E. Wolf, Principles of Optics, Pergamon Press, London, 1968.
[2] H. Kronmüller, Micromagnetism and microstructure of amorphous alloys, Journal of Applied Physics 52 (1981) 1859-1864.
[3] H. Kronmüller, Micromagnetism in amorphous alloys, IEEE Transactions on Magnetics 15, 1979.
[4] M. Vázquez, W. Fernengel, H. Kronmüller, Approach to magnetic saturation in rapidly quenched amorphous alloys, Physica Status Solidi 115/2 (1989) 547-553.
[5] H. Kronmüller, M. Fahnle, Micromagnetism and the microstructureof ferromagnetic solis, Cambridge University Press, 2003.
[6] M. Hischer, R. Reisser, R. Würschum, H.E. Schaefer, H. Kronmüller, Magnetic after-effect and approach to ferromagnetic saturation in naocrystaline iron, Journal of Magnetism and Magnetic Materials 146/1-2 (1995) 117-122.
[7] N. Lenge, H. Kronmüller, Low Temperature Magnetization of Sputtered Amorphous Fe-Ni-B Film, Physica Status Solidi 95/2 (1986) 621-633.
[8] H. Grimm, H. Kronmüller, Investigations of structural defects in the amorphous ferromagnetic alloy$Fe_{40}Ni_{40}P_{14}B_6$, Physica Status Solidi 117/2 (1983) 663-674.

[9] H. Kronmüller, General micromagnetic theory, Publishing House John Wiley and Sons, 2007.
[10] J. Zbroszczyk, Magnetization process and microstructure in the $Fe_{73.5}Cu_1Si_{13.5}B_9$ alloy, Physica Status Solidi 136/2 (1993) 545-554.
[11] J. Zbroszczyk, J. Świerczek, W. Ciurzyńska, M. Baran, B. Wysłocki, S. Szymura, Approach to magnetic saturation in amorphous Co-Fe-Si-B ribbons after surface and heat treatment, Journal of Magnetism and Magnetic Materials 109/2-3 (1992) 221-227.